Mapping daily snow/ice shortwave broadband albedo from Moderate Resolution Imaging Spectroradiometer (MODIS): The improved direct retrieval algorithm and validation with Greenland in situ measurement

Shunlin Liang
Department of Geography, University of Maryland at College Park, College Park, Maryland, USA

Julienne Stroeve
National Snow and Ice Data Center/Cooperative Institute for Research in Environmental Sciences (NSIDC/CIRES), University of Colorado, Boulder, Colorado, USA

Jason E. Box
Department of Geography, Byrd Polar Research Center, Ohio State University, Columbus, Ohio, USA

Received 6 October 2004; revised 29 December 2004; accepted 14 March 2005; published 26 May 2005.

[1] Snow/ice albedo is a critical variable in surface energy balance calculations. The Moderate Resolution Imaging Spectroradiometer (MODIS) data have been used routinely to provide global land surface albedo. The MODIS algorithm includes atmospheric correction, surface reflectance angular modeling, and narrowband to broadband albedo conversion. In an earlier study, a ''direct retrieval'' methodology was proposed to calculate instantaneous albedo over snow and ice-covered surfaces directly from top-of-atmosphere (TOA) MODIS reflectance data. The method consists of extensive radiative transfer simulations for a variety of atmospheric and surface snow conditions and links the TOA reflectance with surface broadband albedo through regression analysis. Therefore the direct retrieval algorithm implicitly incorporates in a single step all three procedures used in the standard MODIS surface albedo algorithm. This study presents improvements to the retrieval algorithm including validation with in situ measurements distributed over the Greenland ice sheet. Comparison with surface observations demonstrates that the direct retrieval algorithm can produce very accurate daily snow/ice albedo with mean bias of less than 0.02 and residual standard error of 0.04.

Citation: Liang, S., J. Stroeve, and J. E. Box (2005), Mapping daily snow/ice shortwave broadband albedo from Moderate Resolution Imaging Spectroradiometer (MODIS): The improved direct retrieval algorithm and validation with Greenland in situ measurement, *J. Geophys. Res.*, *110*, D10109, doi:10.1029/2004JD005493.

1. Introduction

[2] Snow/ice albedo, the surface hemispheric reflectivity integrated over the solar spectrum, is a fundamental component needed for determining the radiation balance of the Earth-atmosphere system. Because of its high albedo, snow and ice allows little solar energy to be absorbed by the surface, and thus plays an important role in regional and global energy balances when snow coverage is variable. In the polar regions, the high surface albedo acts to cool the lower troposphere constituting a critical factor in energy and heat exchange between the poles and the midlatitudes. Even small changes in snow/ice albedo can greatly change the amount of surface absorption without any change in the areal extent of the snow cover [*Nolin and Stroeve*, 1997; *Stroeve et al.*, 1997]. Therefore accurate determination of snow/ice albedo remains an important objective in environmental research and monitoring.

[3] Previous studies have had some success in computing surface albedo from the Advanced Very High Resolution Radiometer (AVHRR) satellite data in polar regions [*De Abreu et al.*, 1994; *Knap and Oerlemans*, 1996; *Stroeve et al.*, 1997; *Key et al.*, 2001; *Stroeve*, 2001]. The AVHRR Polar Pathfinder Program provides gridded maps of the surface albedo for the Arctic and Antarctic at 5-km spatial resolution spanning 1981–2000 [*Maslanik et al.*, 1998; *Key et al.*, 2002]. *Stroeve and Nolin* [2003] used MODIS (Moderate Resolution Imaging Spectroradiometer) Level 1B data to derive the albedo over Greenland. However, the accuracy recommended by *Barry* [1985] of 0.02 for snow albedo still has not been achieved.

[4] The MODIS instrument on board both the Terra and Aqua satellites has been used to map global albedo

0148-0227/05/2004JD005493$09.00

since December 1999. MODIS has improved spectral/spatial characteristics and measurement precision as compared to AVHRR, and therefore it is anticipated to more accurately map surface albedo. Global surface broadband albedo is one of the standard EOS (Earth Observing System) products that has been generated routinely from MODIS data every 16 days (the MOD43 product). The instrument algorithm for generating global land surface albedo from MODIS observations consists of three basic steps [*Lucht et al.*, 2000; *Schaaf et al.*, 2002]: (1) atmospheric correction that converts TOA (top of the atmosphere) radiance to surface directional reflectance; (2) "kernel" angular modeling that converts accumulated 16-day surface directional reflectance to narrowband albedos; and (3) narrowband to broadband conversion that converts narrowband reflectance to broadband albedo.

[5] In principle, the MODIS instrument algorithm for surface albedo is primarily suitable for dense vegetation surfaces because it relies on atmospherically corrected surface reflectance. The MODIS atmospheric correction algorithm depends on the MODIS aerosol retrieval algorithm that in turn depends on the existence of dense vegetation. The MODIS albedo retrieval algorithm accumulates atmospherically corrected surface reflectance during the 16-day period and then fits the reflectances to an empirical BRDF (bidirectional reflectance distribution function) model for calculating the broadband albedo. In a recent validation study, *Stroeve et al.* [2005] found that the MOD43 albedo product retrieves snow/ice albedo over Greenland that are generally within 6% of the in situ station measurements. However, the MOD43 algorithm failed over the more heterogeneous surfaces observed in the ablation region. Furthermore, even at the more homogenous high elevations, the MOD43 albedo tended to underestimate the in situ albedo.

[6] Several efforts have produced daily albedo MODIS products. *Klein and Stroeve* [2002] developed a prototype snow albedo algorithm that also relies on MODIS atmospherically corrected surface reflectance but accounts for reflectance anisotropy using the discrete-ordinate radiative transfer (DISORT) model. *Liang et al.* [1999] developed a direct retrieval algorithm that links TOA narrowband albedo with land surface broadband albedo using a feed-forward neural network. Since the TOA observations contain information on both surface reflectance and atmospheric optical properties, it implies that it is possible to predict surface broadband albedo using TOA narrowband albedos without performing any aerosol corrections, discussed later. The direct retrieval algorithm is designed to work over any surface type, and is particularly well suited for nonvegetated surfaces. The algorithm of *Liang et al.* [1999] was later revised and applied to MODIS data [*Liang*, 2003], but had not been validated over snow/ice surfaces.

[7] Therefore the main objectives of this paper are: (1) to document both the new developments of the direct retrieval algorithm and (2) to present comparisons of the algorithm-derived albedo with in-situ measurements of albedo over a generally homogeneous target, i.e., the Greenland ice sheet. The outline of the direct retrieval algorithm and its improvements are presented in section 2. The validation results are discussed in section 3.

2. Direct Retrieval Algorithm

[8] The current MODIS albedo retrieval is based on a physical understanding of most atmospheric and surface processes. Using a physical approach as such, the albedo will depend on the performance of all the procedures that characterize the known processes, such as performance of the atmospheric correction and the accuracy of the angular model used to describe the directional distribution of the reflectance. It is unknown whether errors associated with each procedure cancel or reinforce each other.

[9] An alternative method to a physically based retrieval is to combine all procedures together in one step through regression analysis. This approach incorporates physical principles through extensive radiative transfer simulations. A fundamental difference in philosophy of the two methods exists, although both methods take into consideration the fact that many variables (e.g., atmospheric properties, surface BRDF, and spectral reflectance) impact the TOA radiance. The MODIS albedo instrument algorithm aims to retrieve most of these variables explicitly, while the direct retrieval algorithm aims only to make a best-estimate broadband albedo. Given the limited amount of observations under normal conditions, we argue that it is easier and likely more accurate to pursue a simplified method that estimates a smaller set of variables (e.g., only broadband albedo) than all the individual variables involved (e.g., aerosol, surface BRDF).

[10] The direct retrieval method primarily consists of two steps [*Liang et al.*, 1999; *Liang*, 2004, 2003]. The first step is to produce a large database of TOA directional reflectance and surface albedo for a variety of surface and atmospheric conditions using radiative transfer model simulations. The second step is to link the simulated TOA reflectance with surface broadband albedo using nonparametric regression algorithms (e.g., neural networks and projection pursuit regression). In earlier work, reflectance spectra of many different land cover types were considered. Since this study focuses only on snow- and ice-covered surfaces, it is possible to replace the nonparametric regression algorithms with parametric regression equations.

[11] However, it is impossible to develop a simple linear regression equation that is suitable for all sun-viewing geometries because of variations in atmospheric and snow/ice properties that affect albedo. Instead, it might be theoretically possible to develop a regression formula as an explicit function of the solar and viewing angles since these angles are known parameters for each observation. After extensive experiments, we unfortunately failed to be able to develop such a universal function. As an alternative, the illumination and viewing hemispheres were divided into many small intervals and a linear equation was developed for each grid element. The concept of the direct retrieval algorithm is illustrated in Figure 1.

2.1. Radiative Transfer Simulation

[12] The purpose of the simulation step is to predict the top of the atmosphere satellite measurement for a variety of atmospheric and surface conditions. The 6S atmospheric

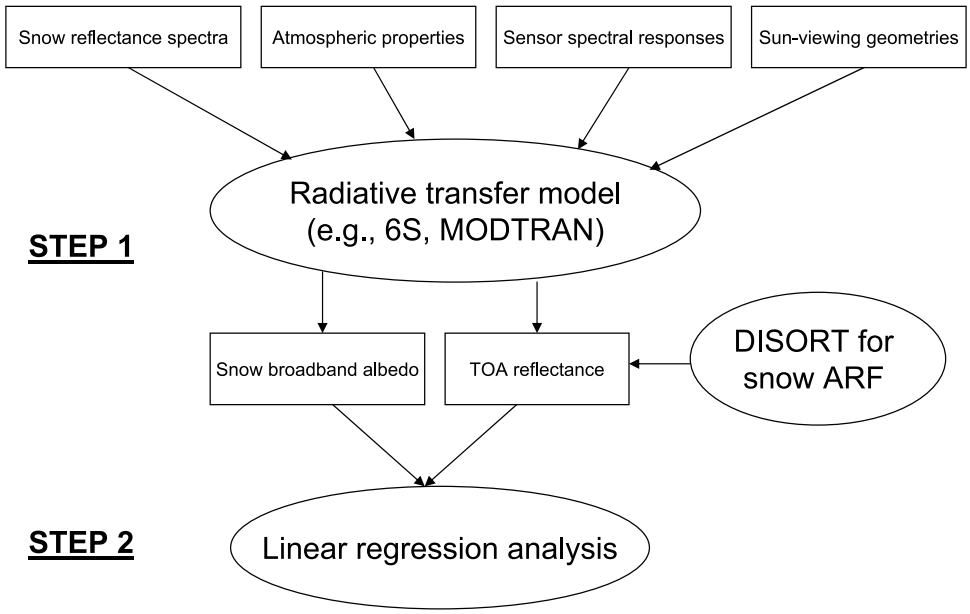

Figure 1. Illustration of the direct retrieval algorithm.

radiative transfer code [*Vermote et al.*, 1997] was used for this purpose. The 6S radiative transfer model allows the user to select from several different atmospheric conditions. In the simulations performed for this study, a rural aerosol model was chosen together with four different aerosol loadings ranging from a clear to a more turbid atmosphere (aerosol optical depth at 550 nm = 0.01, 0.05, 0.1, and 0.2). In addition, a 1976 U.S. standard atmosphere profile was selected. Then 6S was run for eight surface elevation values ranging from 0 to 3500 m at an increment of 500 m. The solar zenith angle was varied from 0° to 85° and the viewing zenith angle from 0° to 75°, both at 5° increments, and the relative azimuth angle from 0° to 180° at every 20°. Since water vapor and ozone amounts can be measured from other channels [e.g., *Kaufman and Gao*, 1992; *Gao and Kaufman*, 2003] and other sensors (e.g., TIROS Operational Vertical Sounder), we did not vary them.

[13] A key element in this procedure is to incorporate different snow reflectance spectra in the procedure to simulate all the possible spectral variations. In total, we used 72 measured snow reflectance spectra available from field experiments that span a variety of surface types, from new snow to bare ice. However, only about one third of the snow reflectance spectra were obtained for the whole hemisphere. Very important is that the melting snow spectra were included. Many of the measured snow reflectance spectra were obtained from the nadir direction and are assumed to be albedo spectra. The error may be introduced by this assumption, but the spectral dependence of these reflectance spectra is the most important property we need since we are mainly interested in surface broadband albedo. In our earlier studies [*Liang et al.*, 1999; *Liang*, 2003], a Lambertian surface was assumed. People always argue about the errors that may be introduced by the Lambertian assumption. In this study, we made efforts to avoid the Lambertian assumption in computing the TOA reflectance. Since the angular properties of snow corresponding to the MODIS channels were not measured, an alternative solution is to simulate the snow bidirectional reflectance factor (BRF) using the DISORT radiative transfer model. DISORT computes the surface BRF for specified viewing and solar geometries, and the corresponding bi-hemispheric reflectance factor (albedo). The ratio of the albedo to the BRF becomes the conversion factor by which the snow reflectance spectrum is multiplied to obtain the angular reflectance spectrum.

[14] In modeling the BRF and albedo, the snow surface is assumed to be composed of spherical homogeneous particles with Gamma size distributions [*Mishchenko et al.*, 1999]. Five mean sizes were specified: 100, 250, 500, 800, and 1000 μm, and the corresponding variances are A/500, where A is the mean particle radius. The optical properties (i.e., single scattering albedo and asymmetry parameter) of snow particles were calculated using a Mie code and then input to the DISORT. The central wavelength was used since our initial experiments indicated the integration into MODIS bands using their spectral response functions does not yield a significant difference. The anisotropic reflectance factor (ARF) for all MODIS bands is calculated from the BRF normalized by the albedo. For the 6S radiative transfer calculations, the measured surface reflectance spectra are multiplied by the corresponding ARF to generate the surface angular reflectance spectra. Note that we did not separate ice from snow in calculating their ARF, which can introduce errors, since ice reflectance is nearly isotropic. However, the ice ARF error is found to be small based on the validation results using ice albedo measurements that are presented later.

[15] It is important to note that we did not use actual surface reflectance spectra with a non-Lambertian surface in 6S TOA reflectance calculations because it would be computationally extremely slow. Instead, the following approximate formula is used to predict TOA reflectance

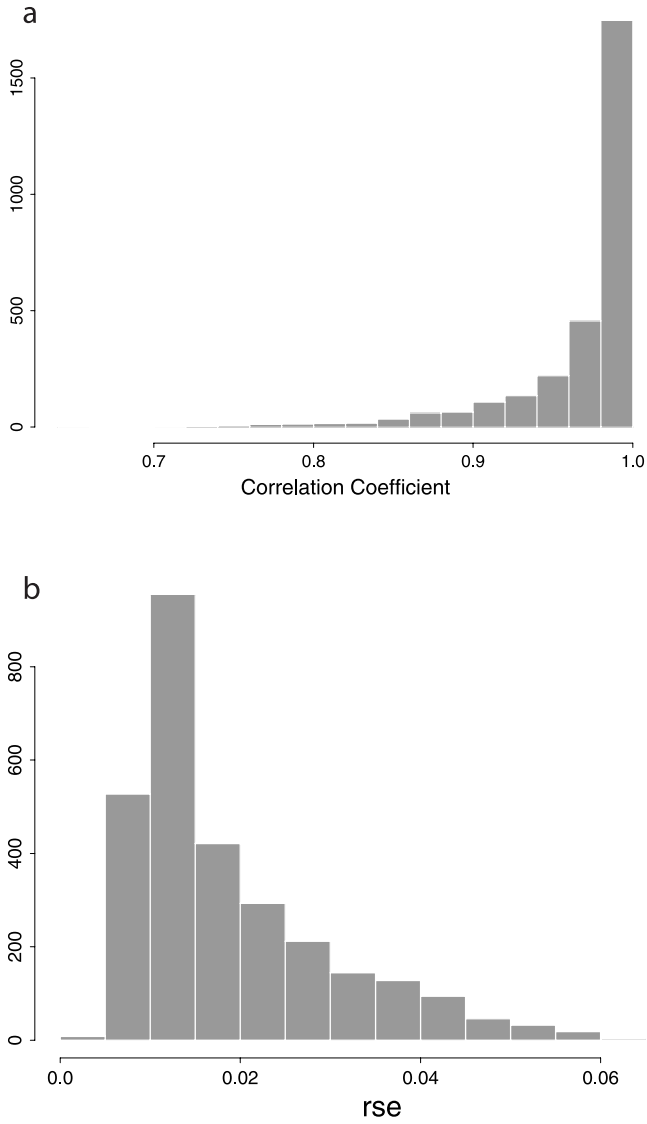

Figure 2. Histograms of (a) multiple R^2 and (b) residual standard error (RSE) of linear regression equation for each angular grid fitted to the simulated TOA reflectance.

($\rho(\tau_t, \mu, \phi)$) with all the atmospheric variables tabulated from the 6S simulations,

$$\rho(\tau_t, \mu, \phi) = t_g \left\{ \rho_0(\tau_t, \mu, \phi) + \gamma(-\mu_0) \left[r_s f(-\mu_0, \mu, \phi) + \frac{r_s \bar{\rho} r_s}{1 - r_s \bar{\rho}} \right] \gamma(\mu) \right\}, \quad (1)$$

where μ_0, μ, and ϕ are, respectively, the cosine of the solar zenith angle, cosine of the viewing zenith angle, and the relative azimuth angle. Here τ_t is aerosol optical depth, t_g is the gaseous transmittance, $\gamma(\mu)$ is the upwelling transmittance, $\gamma(-\mu_0)$ is the downwelling transmittance, ρ is the atmospheric spherical albedo, ρ_0 (τ_t, μ, ϕ) is the atmospheric (path) reflectance without the contributions from the surface, r_s is the surface isotropic albedo, and $f(\cdot)$ is the surface ARF. Note that γ, $\bar{\rho}$, and ρ_0 all depend on aerosol optical depth. The downward irradiance spectra at the surface from the 6S simulations are then integrated with the measured snow reflectance spectra to calculate the surface broadband albedo in the simulation part.

2.2. Linear Regression Analysis

[16] After the database of TOA reflectance and surface albedo is created from the simulations described above, the next step is to link the TOA reflectance to surface broadband albedo. In previous studies [*Liang et al.*, 1999; *Liang*, 2003], a neural network was used to address the high-degree of nonlinearity between the two variables. In this study, we aim to develop an explicit linear regression equation. After extensive experiments, we found it impossible to find a universal linear regression equation suitable for all surface and atmospheric conditions at different sun-viewing geometries. However, the MODIS solar and viewing angles for each pixel are precisely known because of the high accuracy of the satellite geolocation (uncertainty of about 50 m in the horizontal direction). Thus it is theoretically possible to develop a linear regression formula for each solar and viewing angle.

[17] Mathematically, surface broadband albedo α (e.g., shortwave albedo from 0.3 to 3.0 μm), is given by

$$\alpha = a_0 + \sum_{i=1}^{n} a_i \rho_i, \quad (2)$$

where ρ_i is the TOA reflectance derived from ρ_i^{TOA}, the TOA reflectance corrected for atmospheric water vapor and ozone absorption,

$$\rho_i = \rho_i^{TOA} / t_g, \quad (3)$$

Here t_g is the atmospheric gaseous transmittance in both the upward and downward directions. If the water vapor and ozone concentrations are known, t_g can be easily calculated using a simple exponential function or from the existing radiative transfer packages, such as MODTRAN or 6S. Since their impacts on the shortwave albedo are relatively small [*Liang*, 2003], we have used the default values in this study.

[18] To speed up computation, the Sun-viewing hemisphere is divided into 2880 angular grids, corresponding to 18 solar zenith angles, 16 viewing zenith angles, and 10 relative azimuth angles. For each angular series, one set of coefficients is provided for the linear equation (2).

[19] To evaluate the robustness of the linear regression models, two different statistical parameters were used: the square value of the correlation coefficient (R^2) and the residual standard deviation (σ). They were provided for each angular grid from least squares regression. Figure 2 shows the histogram of these two measures. The median values of R^2 and σ are 0.9865 and 0.0145. Figure 3 shows the angular distributions of these two parameters at a relative azimuth angle of 0°. The errors increase with increased solar or viewing zenith angle. Overall, the fitting can be considered to provide excellent results.

3. Validation Results

[20] This section examines the accuracy of the direct retrieval algorithm through comparisons with albedo data

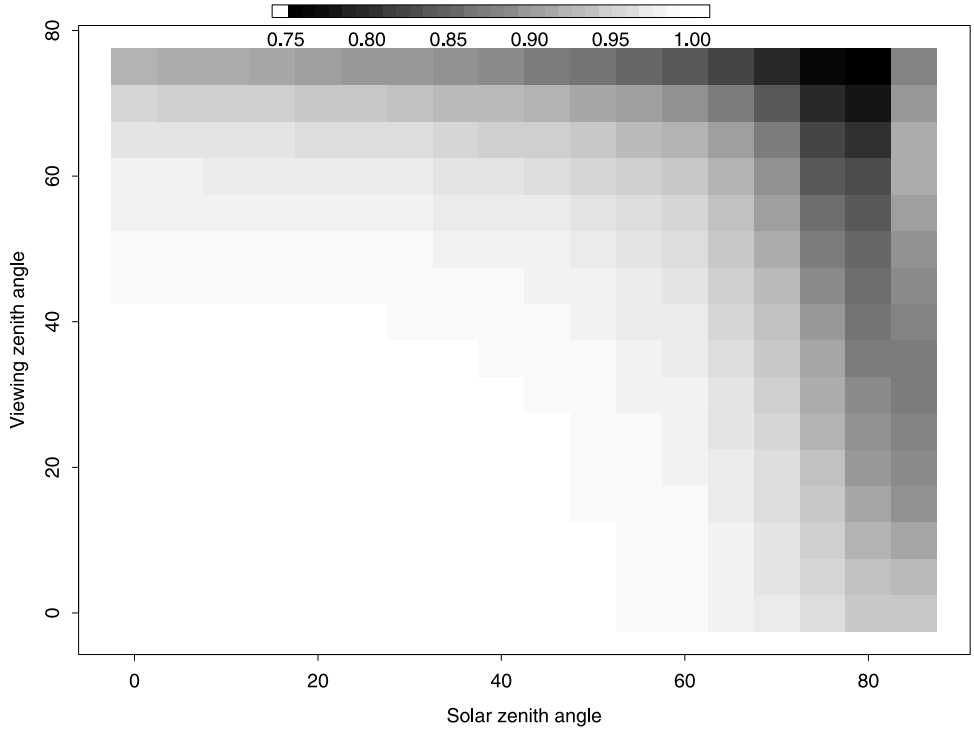

Figure 3. Two-dimensional distribution of the multiple R^2 of linear regression equation at each angular bin fitted to the simulated TOA reflectance when the relative azimuth angle is zero.

collected at automatic weather stations (AWS) distributed widely across the Greenland ice sheet [*Steffen and Box*, 2001]. Downward and upward broadband shortwave radiation fluxes are measured at these Greenland Climate Network (GC-Net) AWS sites using LI-COR 200SZ photoelectric diode pyranometers and provide hourly albedo estimates. The limited spectral sensitivity (0.4–1.1 μm) of the LI-COR 200SZ has necessitated correction developed based on comparisons of LI-COR 200SZ observations with standard optical black thermopile instruments that measure in the 0.285–2.8 μm range. The correction method was used in a recent MODIS 16-day albedo product validation study [*Stroeve et al.*, 2005] to yield full broadband albedo data with ±0.03 uncertainty.

[21] Measurements at five stations (Table 1) during 2002 were used in this study. These stations were chosen as they represent an elevation transect from the melt region near the western margin of the ice sheet up to the dry snow zone. These stations therefore allow for an examination of how well the algorithm works over not only homogeneous snow but also over heterogeneous melting conditions. Channels 1 through 7 MODIS level 1B data for 2000 (from collection 4) were gridded to a 1.25 km EASE-grid [*Armstrong et al.*, 1997]. Clear-sky MODIS scenes were first selected by visible inspection of the MODIS imagery. A further check on whether or not the AWS was cloud-free for the selected MODIS orbit was performed by comparing observed incoming solar irradiance with modeled clear-sky irradiance calculations from the FluxNet radiative transfer model [*Key and Schweiger*, 1998]. Effective cloud transmission (T_e) is defined as the ratio of the measured incoming solar radiation to that computed by the radiative transfer model. A value near 1.0 implies clear sky conditions. Note that an increase in diffuse sky irradiance in the presence of thin clouds will act to underestimate true cloud amount. However, we aim only to discriminate between cloudy and noncloudy using a threshold of $T_e > 0.8$ to indicate clear sky conditions for selection of cloud free MODIS data over the AWS locations. Errors of falsely attributing a cloudy observation site as clear represent a minority of cases.

[22] Figures 4–8 show the comparisons of MODIS-retrieved broadband albedo and in situ observations at the five sites. The retrieved MODIS albedo represents the average albedo of all pixels in an 11 × 11 pixel window

Table 1. Station Names and Locations From the Greenland Automatic Weather Stations (AWS) Used in This Study

Station ID Number	Site Name	Latitude, °N	Longitude, °W	Elevation, m	Activation Date (Decimal)
1	Swiss Camp	69.5732	49.2952	1149	1995.00
2	CP1	69.8819	46.9763	2022	1995.39
6	Summit	72.5794	38.5042	3208	1996.37
9	JAR1	69.4984	49.6816	962	1996.47
17	JAR2	69.4200	50.0575	568	1999.41

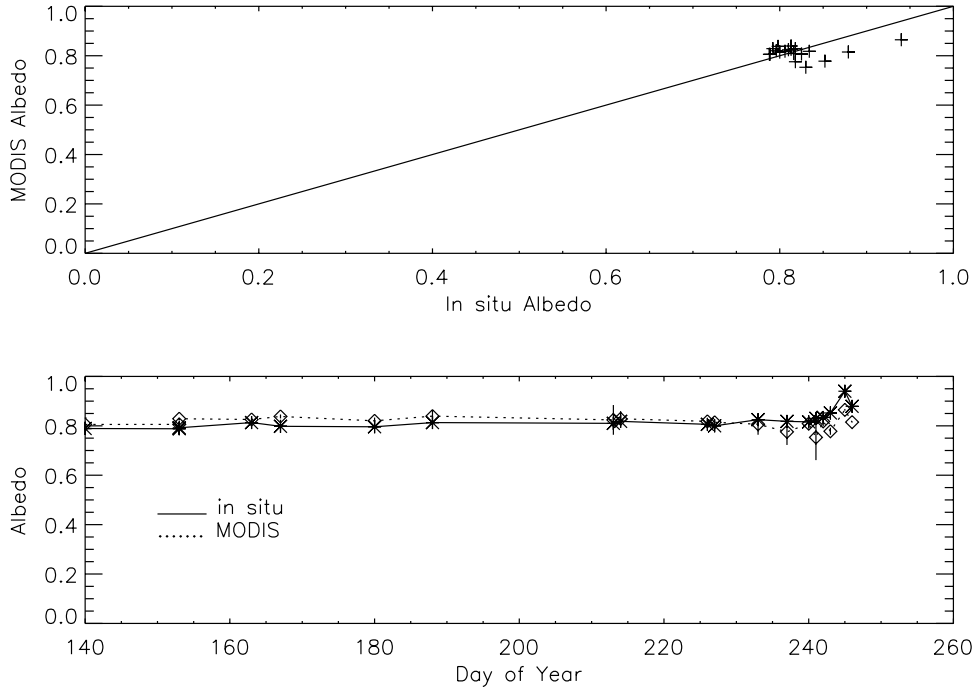

Figure 4. Comparison of the retrieved snow broadband albedo with the ground measurements at site Summit.

around each station. Because of the geolocation error and other uncertainties in the MODIS data (e.g., sub-pixel clouds), we did not use the central pixel only. It is evident from these figures that there is an excellent agreement at all sites except JAR1. It is not surprising since station JAR1 is located in the ablation region of the ice sheet and surface heterogeneity (e.g., melt ponds, cracks and crevasses, cryoconite dust concretions, and rough surface features) complicates the comparison between the satellite and ground-based point measurements. Perennial melt lakes

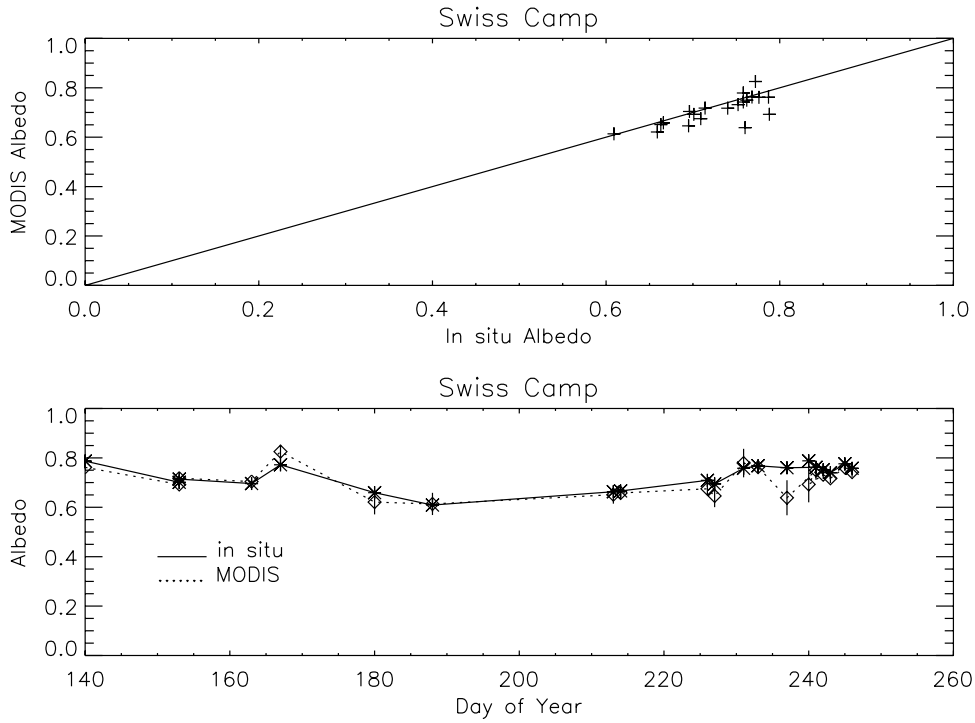

Figure 5. Comparison of the retrieved snow broadband albedo with the ground measurements at site Swiss Camp.

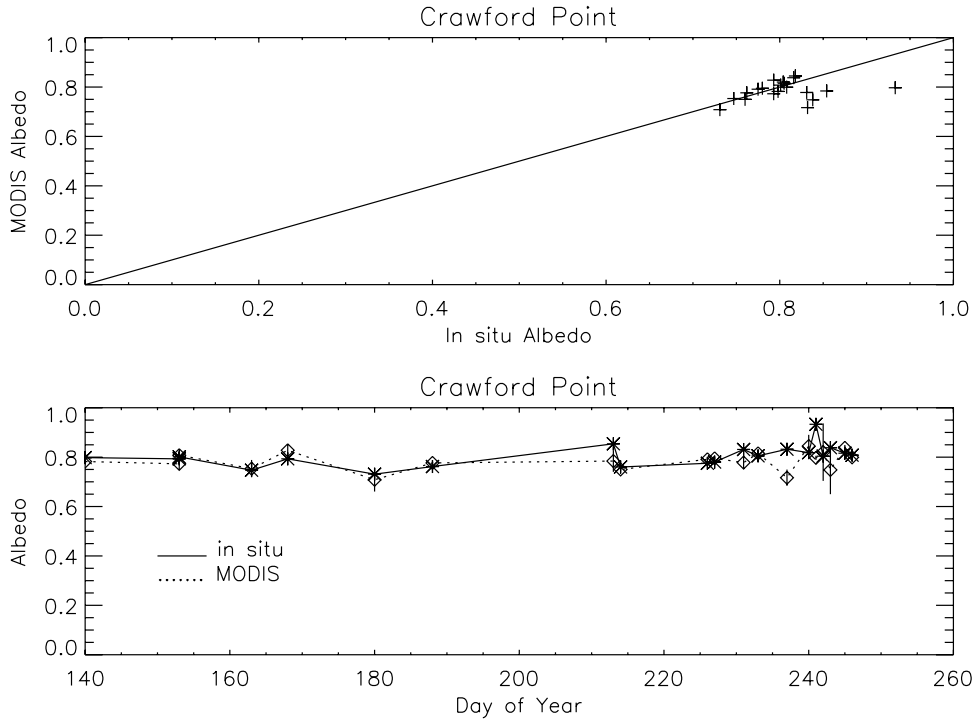

Figure 6. Comparison of the retrieved snow broadband albedo with the ground measurements at site CP1.

occur in the vicinity of JAR1, flooding the site for several days in 1996 and 1997. Note that a systematic bias still exists seemingly because of the mismatch of the ground "point" measurement with the MODIS 1-km pixel. The ground observation measurement footprint is approximately 4 m^2, but instrument height varies from 1.5 m to 4 m with ice ablation and seasonal snow accumulation. It is interesting to note that JAR2 is also quite heterogeneous, but the

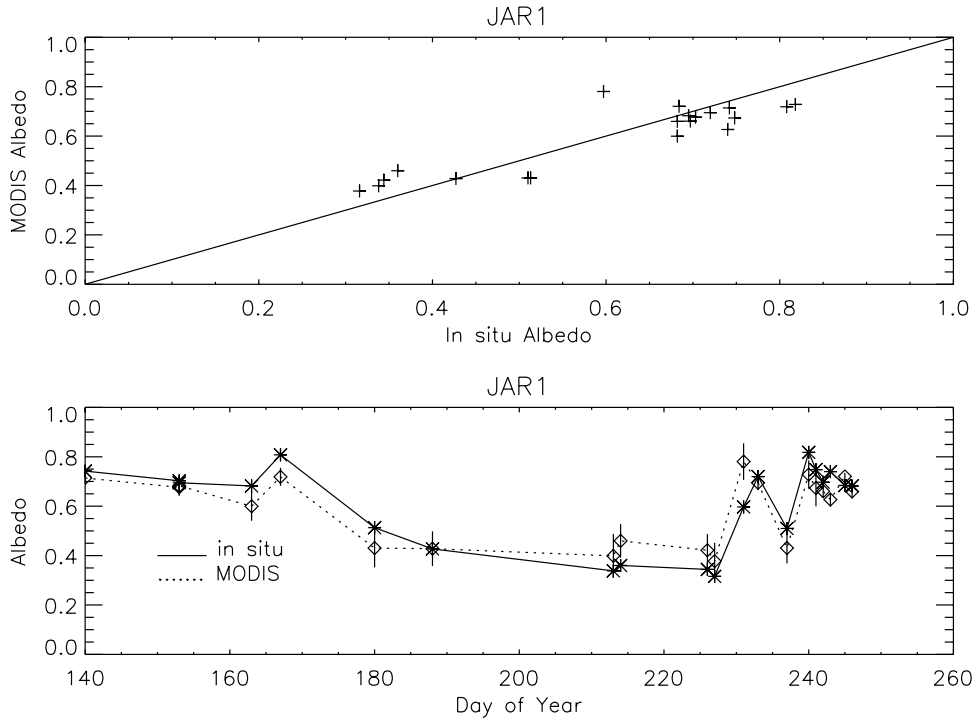

Figure 7. Comparison of the retrieved snow broadband albedo with the ground measurements at site JAR1.

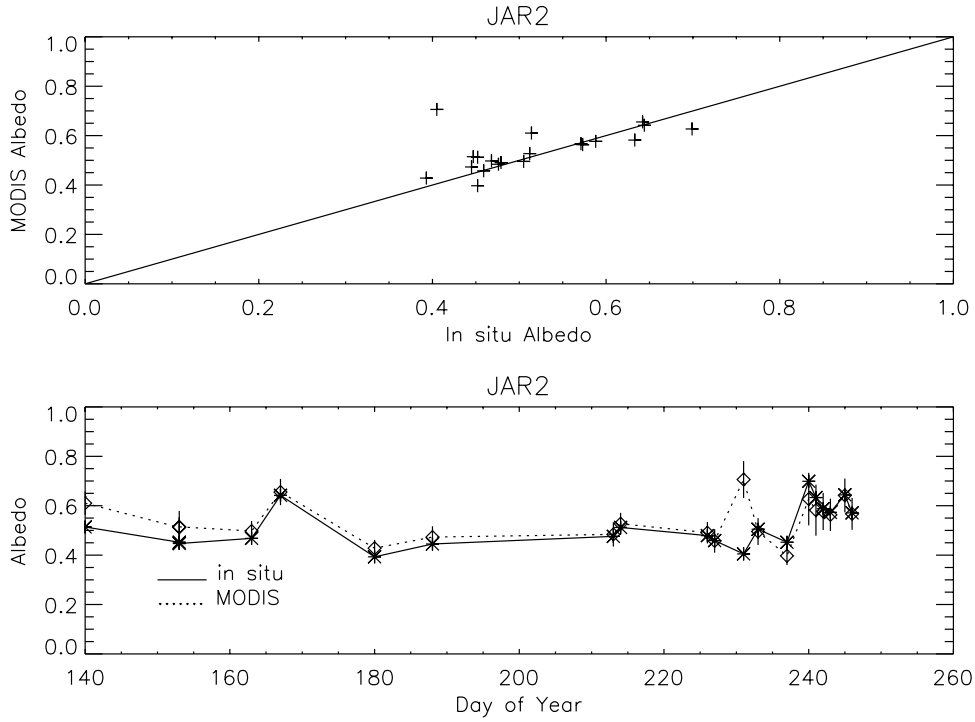

Figure 8. Comparison of the retrieved snow broadband albedo with the ground measurements at site JAR2.

comparison of the mean values between the observed and the retrieved is very good, implying a calibration or an otherwise unknown error at JAR1.

[23] Table 2 shows the differences of the mean values, which are a reasonably good indicator of any biases between the measured and the retrieved, and the residual standard error between the measured and the retrieved albedo values. At JAR2, the observation on day 231 was excluded in the calculation since the MODIS pixel had a cloudy or partially cloudy texture. If we exclude JAR1, the differences of the mean values are smaller than 0.02, and the residual standard error is about 0.04. We may argue that the actual accuracy of the albedo product using our retrieval method will be better since we have compared the ground "point" measurements with the retrieved albedo of a region around each site. Any sub-pixel clouds and surface heterogeneity of MODIS pixels still affect the retrieved albedo value. The procedure for converting the spectrally narrow measured to broadband shortwave albedo might also contribute to the uncertainty. Further, observational errors due to rime formation and inadequate and instrument leveling can be significant, though they are difficult to estimate with site visits only once per year.

[24] A key advantage of the direct-retrieval algorithm is its simplicity in routine implementation. It involves only a linear transformation for each pixel, and therefore it is computationally efficient. For illustration purposes, Figure 9 is a color composite of MODIS imagery over Greenland that was acquired on 17 June 2002. The image is gridded to the 1.25-km EASE-grid with dimensions of 1860 by 1740. The western slope of the Greenland ice sheet where the largest areas of melting occur is mostly clear of clouds. The retrieved shortwave albedo using the direct-

Table 2. Validation Results Summary

Station	Mean Difference	Residual Standard Error
Swiss Camp	0.019	0.033
CP	0.015	0.043
Summit	−0.005	0.036
JAR1	0.023	0.078
JAR2	−0.008	0.042

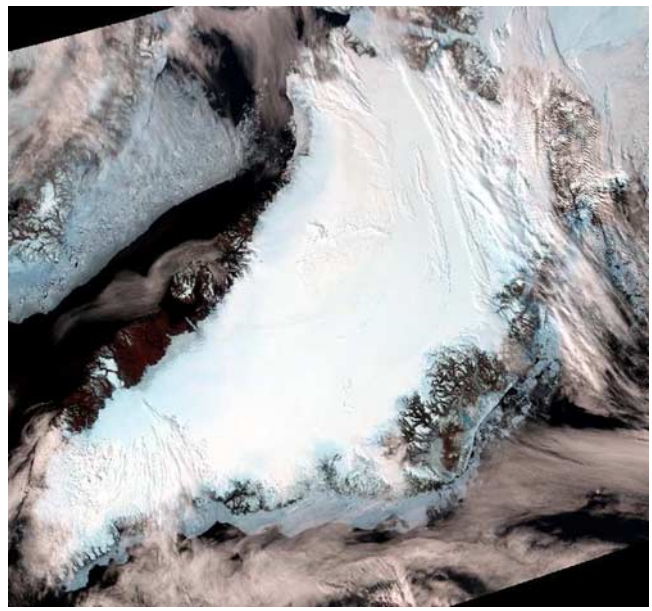

Figure 9. Example color composite MODIS image over Greenland, acquired on 17 June 2002.

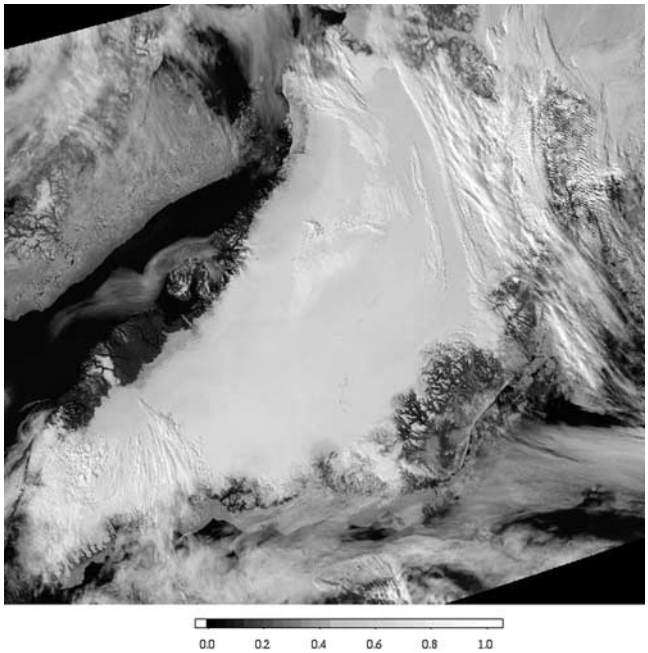

Figure 10. Retrieved instantaneous broadband albedo map from the image shown in Figure 9.

retrieval algorithm is shown in Figure 10 and does not include any obvious outliers. It is indeed shown that along the ice sheet margins the snow albedo varies dramatically whereas the central region from the lower left to the upper right has constant high albedo values.

4. Summary

[25] Snow albedo is a critical variable to assess the surface radiation budget in energy balance models based on satellite data assimilation [e.g., *Box et al.*, 2004]. The MODIS data have been used to map global land surface albedo every 16 days routinely [*Lucht et al.*, 2000; *Schaaf et al.*, 2002]. A beta version of a daily snow albedo product [*Klein and Stroeve*, 2002] is also available right now. The direct retrieval method for mapping daily albedo was published earlier [*Liang et al.*, 1999; *Liang*, 2003, 2004], but some significant revisions for calculating snow albedo and validation results using in situ measurements were presented in this study.

[26] The most important improvement to the direct-retrieval algorithm is that the nonparametric regression method (e.g., neural network) used in the previous studies has been replaced by an explicit multiple linear regression analysis in the current study. Another important improvement is that the Lambertian assumption used in the previous study has been replaced with a more explicit snow BRDF model. A key improvement is the inclusion of angular grids that represent reflectance over the entire Sun-viewing angular hemisphere. A linear regression equation is developed for each grid, and thus thousands of linear equations are developed in this algorithm for converting TOA reflectance to surface broadband albedo directly.

[27] Measurements from Greenland Climate Network (GC-Net) Automatic Weather Stations (AWS) have been used to validate the accuracy of this algorithm. Excellent agreements were found, and for all of the five stations used, the average difference is smaller than 0.02. Note that there exist several exogenous error sources in this validation procedure, i.e., ground observation error and a scale gap comparing 4 m^2 ground observations with 10^6 m^2 MODIS pixels that do not resolve spatial inhomogeneities with a length scale smaller than 1000 m. In situ observational errors also produce an uncertainty limit of ±0.03 that the MODIS data seem to outperform.

[28] The snow BRDF is based on a model calculation. Further study is warranted to incorporate observationally based snow surface BRDFs at MODIS spectral intervals, either from satellite observations (e.g., MODIS/MISR) retrieval or including more factors (e.g., surface roughness) into this algorithm. However, it appears that the spectral information is more important than the angular information in estimating broadband albedo from MODIS.

[29] Surface elevation is explicitly incorporated into the model simulation, but the interactions of surface slopes have not been taken into account. The uncertainty needs to be fully evaluated, and topographic correction may be developed in the future. We also propose to correct for water vapor and ozone effects using external data sources. The impacts of the uncertainties of these products on the surface albedo products also need to be evaluated.

[30] The algorithm is very simple and suitable for being implemented to map daily snow albedo globally from MODIS although additional testing and validations are always needed. When routinely implementing this algorithm for processing MODIS data, the MODIS cloud mask product may be useful to exclude the cloud-contaminated pixels. If the cloud mask product is not reliable over snow/ice surfaces, it may be possible to "flag" the pixels with a sudden albedo change since clouds tend to vary more dramatically than snow/ice surfaces.

[31] Finally, this algorithm is suitable to estimate global shortwave albedo of nonvegetated surfaces for the Visible/Infrared Imager/Radiometer Suite (VIIRS), the primary visible and infrared sensor to be flown onboard the platforms of the National Polar-orbiting Operational Environmental Satellite System (NPOESS) and the NPOESS Preparatory Project (NPP) in 2008.

[32] **Acknowledgments.** We would like to thank Feng Gao, Dorothy Hall, Andrew Klein, Ann Nolin, and Crystal Schaaf for their valuable discussions and inputs in the early stage of this study. We also thank Konrad Steffen for leading the Greenland Climate Network automatic weather station effort, and anonymous reviewers for their valuable comments that greatly improve the presentation of this paper. This work was supported with NASA funding.

References

Armstrong, R., M. J. Brodzik, and A. Varani (1997), The NSIDC ease-grid: Addressing the need for a common, flexible, mapping and gridding scheme, *Earth Syst. Monit.*, *7*(4), 3 pp.

Barry, R. G. (1985), Detecting the climate effects of increasing CO_2, *DOE/ER-0235*, pp. 109–141, Dep. of Energy, Washington, D. C.

Box, J. E., D. H. Bromwich, and L. S. Bai (2004), Greenland ice sheet surface mass balance for 1991–2000: Application of polar MM5 mesoscale model and in situ data, *J. Geophys. Res.*, *109*, D16105, doi:10.1029/2003JD004451.

De Abreu, R. A., J. Key, J. Maslanik, M. C. Serreze, and E. F. LeDrew (1994), Comparison of in situ and AVHRR-derived broadband albedo over arctic sea ice, *Arctic*, *147*, 288–297.

Gao, B. C., and Y. J. Kaufman (2003), Water vapor retrievals using Moderate Resolution Imaging Spectroradiometer (MODIS) near-infrared

channels, *J. Geophys. Res.*, *108*(D13), 4389, doi:10.1029/2002JD003023.
Kaufman, Y., and B. C. Gao (1992), Remote sensing of water vapor in the near IR from EOS/MODIS, *IEEE Trans. Geosci. Remote Sens.*, *30*, 871–884.
Key, J., and A. J. Schweiger (1998), Tools for atmospheric radiative transfer: Streamer and FluxNet, *Comput. Geosci.*, *24*, 443–451.
Key, J., X. Wang, J. Stroeve, and C. Fowler (2001), Estimating the cloudy sky albedo of sea ice and snow from space, *J. Geophys. Res.*, *106*, 12,489–12,497.
Key, J., C. Fowler, J. Maslanik, T. Haran, T. Scambos, and W. Emery (2002), *The Extended AVHRR Polar Pathfinder (app-x) Product*, version 1.0 [CD-ROM], Space Sci. and Eng. Cent., Univ. of Wisc., Madison.
Klein, A. G., and J. Stroeve (2002), Development and validation of a snow albedo algorithm for the MODIS instrument, *Ann. Glaciol.*, *34*, 45–52.
Knap, W. H., and J. Oerlemans (1996), The surface albedo of the Greenland ice sheet: Satellite-derived and in situ measurements in the Sondre Stromfjord area during the 1991 melt season, *J.*, *42*, 364–374.
Liang, S. (2003), A direct algorithm for estimating land surface broadband albedos from MODIS imagery, *IEEE Trans. Geosci. Remote Sens.*, *41*, 136–145.
Liang, S. (2004), *Quantitative Remote Sensing of Land Surfaces*, 534 pp., John Wiley, Hoboken, N. J.
Liang, S., A. Strahler, and C. Walthall (1999), Retrieval of land surface albedo from satellite observations: A simulation study, *J. Appl. Meteorol.*, *38*, 712–725.
Lucht, W., C. B. Schaaf, and A. H. Strahler (2000), An algorithm for the retrieval of albedo from space using semiempirical BRDF models, *IEEE Trans. Geosci. Remote Sens.*, *38*, 977–998.
Maslanik, J., C. Fowler, J. Key, T. Scambos, T. Hutchinson, and W. Emery (1998), AVHRR-based polar pathfinder products for modeling applications, *Ann. Glaciol.*, *25*, 388–392.
Mishchenko, M. I., J. M. Dlugachb, E. G. Yanovitskijb, and N. T. Zakharovac (1999), Bidirectional reflectance of flat, optically thick particulate layers: An efficient radiative transfer solution and applications to snow and soil surfaces, *J. Quant. Spectrosc. Radiat. Transfer*, *63*, 409–432.
Nolin, A. W., and J. C. Stroeve (1997), The changing albedo of the Greenland ice sheet: Implications for climate change, *Ann. Glaciol.*, *25*, 51–57.
Schaaf, C., et al. (2002), First operational BRDF, albedo nadir reflectance products from MODIS, *Remote Sens. Environ.*, *83*, 135–148.
Steffen, K., and J. E. Box (2001), Surface climatology of the Greenland ice sheet: Greenland climate network 1995–1999, *J. Geophys. Res.*, *106*, 33,951–33,964.
Stroeve, J. (2001), Assessment of Greenland albedo variability from the advanced very high resolution radiometer Polar Pathfinder data set, *J. Geophys. Res.*, *106*, 33,989–34,006.
Stroeve, J., and A. Nolin (2003), Comparison of MODIS and MISR-derived surface albedo with in situ measurements in Greenland, *EARSeL eProc.*, *2*(1), 88–96.
Stroeve, J., A. Nolin, and K. Steffen (1997), Comparison of AVHRR-derived and in-situ surface albedo over the Greenland ice sheet, *Remote Sens. Environ.*, *62*, 262–276.
Stroeve, J., J. Box, F. Gao, S. Liang, A. Nolin, and C. Schaaf (2005), Accuracy assessment of the MODIS 16-day snow albedo product: Comparisons with Greenland in situ measurements, *Remote Sens. Environ.*, *94*, 46–60.
Vermote, E., D. Tanre, J. L. Deuze, M. Herman, and J. Morcrette (1997), Second simulation of the satellite signal in the solar spectrum: An overview, *IEEE Trans. Geosci. Remote Sens.*, *35*, 675–686.

J. E. Box, Department of Geography, Byrd Polar Research Center, Ohio State University, Columbus, Ohio, USA.
S. Liang, Department of Geography, University of Maryland at College Park, College Park, MD 20742, USA. (sliang@geog.umd.edu)
J. Stroeve, National Snow and Ice Data Center/Cooperative Institute for Research in Environmental Sciences (NSIDC/CIRES), University of Colorado, Boulder, Colorado, USA.